Guided-wave optical pressure sensor with semi-closed space under the diaphragm: step response in relation to the area of a small hole of a semi-closed space

Kaoru Sato[a], Masashi Ohkawa[b], Seishi Sekine[b], and Takashi Sato[b]
[a] Graduate School of Science and Technology, Niigata University
8050 Ikarashi 2-no-cho, Niigata 950-2181, Japan
[b] Faculty of Engineering, Niigata University
8050 Ikarashi 2-no-cho, Niigata 950-2181, Japan

ABSTRACT

An original guided-wave optical pressure sensor, which has a semi-closed space with a small hole under a diaphragm, can be used even under high quasi-static pressure without sacrificing sensitivity, unlike conventional pressure sensors. Moreover, the sensor possesses characteristics of a high-pass filter, so that it responds to only the high-frequency components of pressure change. The cutoff frequency of the high-pass filter of the sensor property is a key factor in designing the sensor, and is acquired from the step response of the sensor. In a step-like change in ambient pressure, a pressure difference is induced on the diaphragm for a short while because the small hole restricts fluid flow between the semi-closed space and the surroundings. The reciprocal of the duration of the induced pressure difference corresponds to the cutoff frequency. In this study, the step response in relation to the cross-sectional area of the small hole was examined experimentally, and the measured durations were compared with the theoretical ones. In the experiment, the duration was approximately inversely proportional to the area of the small hole as theoretically predicted although the measured durations are larger by a factor of thousands than the calculated ones.

1. INTRODUCTION

Since an integrated optic temperature sensor was demonstrated by L. M. Johnson et al. in 1981 [1], the guided-wave optical sensors have steadily attracted attentions due to following excellent advantages: miniaturization feasibility, alignment-free configuration, and potentially efficient interaction between the lightwave and the measurand. In addition, due to immunity to electromagnetic interference and impossibility of electrical leak, the sensors can be applied even in harsh environments, such as industrial plants, nuclear power plants, etc.

Our group has been developing glass-based and silicon-based guided-wave optical pressure sensors with diaphragms.[2,3] Also, several groups have reported on integrated optic pressure sensors with micro-machined diaphragms.[4,5] In such pressure sensors, high sensitivity is not generally compatible with high proof pressure. Therefore, the conventional sensors with high sensitivity cannot be used under high pressure, greatly limiting the sensing range to relatively low pressure cases. However, detection of small pressure fluctuation under high pressure is desired in some applications, *e.g.* monitoring for malfunctions in static-high-pressure pipelines of industrial plants, observation of tidal waves which cause hydraulic pressure changes on the bottom of the sea, etc.

Our original guided-wave optical pressure sensor has a semi-closed space with a small hole under a diaphragm, and can be used even under high quasi-static pressure without sacrificing sensitivity. In static pressure, since the small hole equalizes the pressures in the surroundings and in the semi-closed space, no pressure difference appears on the diaphragm even in high ambient pressure. In a step-like change in ambient pressure, pressure in the semi-closed space cannot quickly adjust due to the small hole restricting fluid flow. So, a pressure difference is induced on the diaphragm for a short while. This means that the sensor works as a kind of high-pass filter. The duration of the induced pressure difference is an important parameter in the sensor since its reciprocal determines the cutoff frequency of the high-pass filter of the sensor property. According to the theoretical consideration, the duration is proportional to the V/A ratio, *i.e.* the ratio of the volume of the semi-closed space and the cross-sectional area of the small hole.[6] In this study, the relationship between the duration and the area of the small hole was examined experimentally. In designing the sensor,

Photonic Applications for Aerospace, Transportation, and Harsh Environments
edited by Anbo Wang, Christopher S. Baldwin, Alex A. Kazemi
Proc. of SPIE Vol. 6379, 637908, (2006) · 0277-786X/06/$15 · doi: 10.1117/12.685977

it is very significant to collect experimental data regarding the duration of the induced pressure difference since present theoretical calculations provide only qualitative estimations because there is little reliable data regarding pressure drop and fluid friction at the small hole.

2. PRINCIPLE OF SENSOR OPERATION

Figure 1 shows a guided-wave optical pressure sensor with a semi-closed space under a diaphragm. The sensor has a thin rectangular diaphragm as a pressure-sensitive structure and a straight single-mode waveguide across the diaphragm. A plate with a small hole is attached to the bottom, so that the semi-closed space is formed under the diaphragm. The semi-closed space with the small hole brings high proof pressure to the sensor under static pressure.
When the sensor is placed under static pressure, the pressure in the surroundings of sensor is equal to that in the semi-closed space because the small hole connects the semi-closed space with the surroundings. In this case, no pressure difference is induced onto the diaphragm. So, the diaphragm is not broken even by high static pressure. On the other hand, while the ambient pressure over the sensor changes quickly, the pressure in the semi-closed space changes at a slower rate due to the small hole restricting fluid flow. This delay creates a pressure difference on the diaphragm. Hence, a pressure difference is induced by the higher rate of change in ambient pressure, and the sensor responds only to high frequency components of the ambient pressure change.
The diaphragm is distorted by the induced pressure difference. The distortion causes strain, which in turn produces a change in the refractive index of the diaphragm by the elasto-optic effect. The index change causes phase retardation in the lightwave, which is propagated in the waveguide on the diaphragm. When the phase retardation is dependent on the guided modes, *i.e.* the fundamental TM-like and TE-like modes, the phase difference between the two modes is also a function of the pressure difference. To detect the phase difference, the sensor is placed in a pair of crossed polarizers. The input polarizer is oriented at 45° with respect to the polarization of each guided mode. The light beam through the input polarizer is coupled to the TM-like and TE-like modes at equal intensities. At the end of the waveguide, the lightwave has linear, elliptic, or circular polarization, corresponding to the induced phase difference between the two guided modes. Finally, the crossed output polarizer converts the polarization-modulated light into intensity-modulated light.

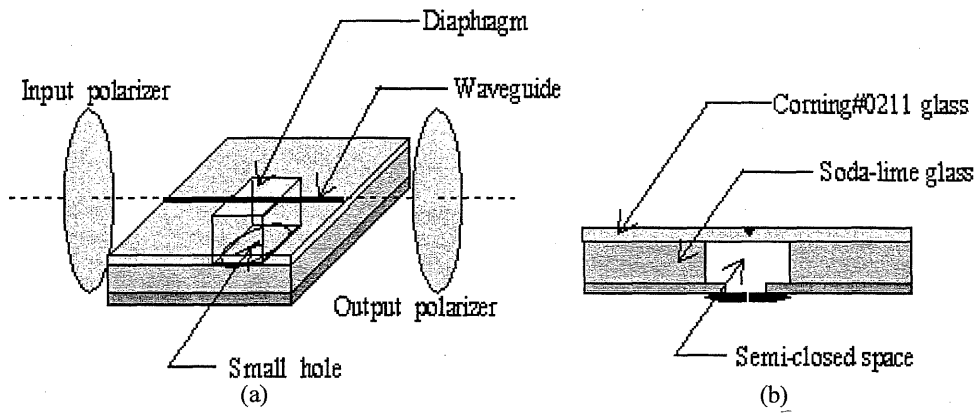

Fig. 1 (a) Schematic drawing of a guided-wave optical pressure sensor with a semi-closed space under a diaphragm, including a pair of crossed polarizers. (b) The cross-sectional view of the sensor

3. THEORY

In designing the sensor, the duration of the induced pressure difference in step response is very significant because its reciprocal corresponds to the cutoff frequency of high-pass filter of the sensor property, as mentioned above. Figure 2 is a drawing of the theoretical model showing how the induced pressure difference $\Delta p(t)$ on the diaphragm in a step-like change in ambient pressure is derived. V and A denote the volume of the semi-closed space and sectional area of the small hole, respectively. In the initial state, that is, immediately after the step-like increase of the ambient pressure from p_0 to p_a, the pressure of the semi-closed space remains p_0, and is written as $p_0 = p_a - \Delta p_0$ using the initial pressure difference Δp_0. After the step-like pressure change, the pressure $p(t)$ in the semi-closed space, written as $p(t) = p_a - \Delta p(t)$, changes as fluid flows into the semi-closed space through the small hole. At $t = 0$, $p(0) = p_0$ and $\Delta p(0) = \Delta p_0$.

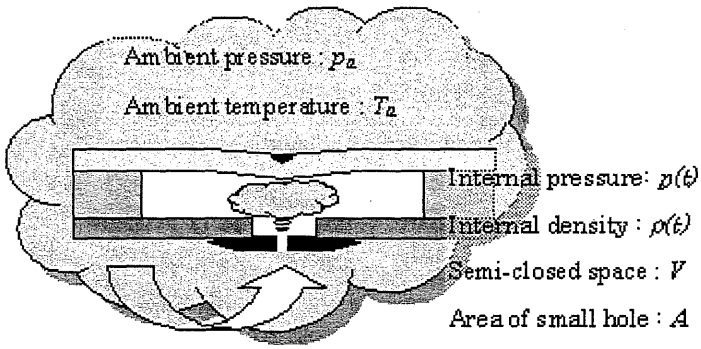

Fig. 2. Drawing of the theoretical model to derive the duration of the induced pressure difference in step response.

From Bernoulli's theorem for compressible fluid, mass flow rate through the small hole is expressed as

$$\dot{m} = \frac{p_a A}{\sqrt{RT_a}} \sqrt{\frac{2\gamma}{\gamma - 1}\left\{\left(\frac{p(t)}{p_a}\right)^{\frac{2}{\gamma}} - \left(\frac{p(t)}{p_a}\right)^{\frac{\gamma+1}{\gamma}}\right\}} = \frac{p_a A}{\sqrt{RT_a}} \sqrt{\frac{2\gamma}{\gamma - 1}\left\{\left(1 - \frac{\Delta p(t)}{p_a}\right)^{\frac{2}{\gamma}} - \left(1 - \frac{\Delta p(t)}{p_a}\right)^{\frac{\gamma+1}{\gamma}}\right\}}, \quad (1)$$

where R is the gas constant and γ is the specific heat. If the induced pressure difference $\Delta p(t)$ is assumed to be much less than the ambient pressure p_a, eq. (1) can be approximately rewritten as

$$\dot{m} = \sqrt{\frac{2p_a}{RT_a}} A \sqrt{\Delta p(t)}\,. \quad (2)$$

Under an assumption of the adiabatic change,

$$\frac{p(t)}{p_0} = \left(\frac{\rho(t)}{\rho_0}\right)^{\gamma}, \quad (3)$$

where $\rho(t)$ denotes the density of the fluid in the semi-closed space, and ρ_0 is the initial value of $\rho(t)$ at $t = 0$. From eq. (3) and $\rho(t) = \rho_0 + \Delta\rho(t)$, if $\Delta\rho(t)$ is much less than ρ_0, the pressure difference can be approximately given by

$$\Delta p(t) = \Delta p_0 - \gamma \frac{p_0}{\rho_0} \Delta\rho(t)\,. \quad (4)$$

Incidentally, from the law of conservation of mass, mass $\dot{m}dt$ of the fluid coming into the semi-closed space during a short period of dt must equal the increased mass $Vd\rho$ in the semi-closed space as follows.

$$\dot{m}dt = Vd\rho = Vd(\Delta\rho)\,. \tag{5}$$

Using the relation between $\Delta p(t)$ and $\Delta\rho(t)$ of eq. (4), eq. (5) can be rewritten as

$$\dot{m}dt = -\frac{\rho_0}{\gamma p_0} Vd(\Delta p)\,. \tag{6}$$

Equation (2) is substituted into eq. (6),

$$\sqrt{\frac{2p_a}{RT_a}} \cdot \frac{\gamma p_0}{\rho_0} \cdot \frac{A}{V} dt = -\frac{1}{\sqrt{\Delta p}} d(\Delta p)\,. \tag{7}$$

Equation (7) is integrated from 0 to t with respect to t on the left side and from Δp_0 to Δp with respect to Δp on the right side. After the definite integral,

$$\sqrt{\frac{2p_a}{RT_a}} \cdot \frac{\gamma p_0}{\rho_0} \cdot \frac{A}{V} t = 2\left(\sqrt{\Delta p_0} - \sqrt{\Delta p(t)}\right). \tag{8}$$

Equation (8) can be rewritten as

$$\sqrt{\Delta p(t)} = \sqrt{\Delta p_0} - \sqrt{\frac{p_a}{2RT_a}} \frac{\gamma p_0}{\rho_0} \frac{A}{V} t\,. \tag{9}$$

When the right side in eq. (9) is positive, the pressure difference is induced on the diaphragm. Therefore, the duration of the induced pressure difference t_d is given by

$$t_d = \sqrt{\frac{2RT_a}{p_a}} \frac{\rho_0}{\gamma p_0} \frac{V}{A} \sqrt{\Delta p_0}\,. \tag{10}$$

From eq. (10), the duration is found to be proportional to the V/A ratio, and proportional to the square root of the initial pressure difference. Within the duration, the pressure difference is expressed as

$$\Delta p(t) = \left(\sqrt{\Delta p_0} - \sqrt{\frac{p_a}{2RT_a}} \frac{\gamma p_0}{\rho_0} \frac{A}{V} t\right)^2. \tag{11}$$

By applying the Laplace transform to eq. (11), the transfer function can be calculated, and is expressed as

$$G(f) = 1 - 2\left(\frac{f_0}{f}\right)^2 \left\{1 - \cos\left(\frac{f}{f_0}\right)\right\} - i\frac{2f_0}{f}\left\{1 - \frac{f_0}{f}\sin\left(\frac{f}{f_0}\right)\right\}, \tag{12}$$

where $i = \sqrt{-1}$, and f_0 is defined as the reciprocal of the duration of the induced pressure difference, *i.e.* $f_0 = 1/t_d$. Figure 3 shows the calculated magnitude $|G(f)|$ and phase $\angle G(f)$ as a function of the normalized frequency f/f_0. It is found from the figure that the sensor has a function of a high-pass filter. The cutoff frequency is $1.57f_0$ or $1.57/t_d$, and the magnitude decreases at a 10 dB/dec or 3 dB/oct slope below the cutoff frequency. The sensor responds, like conventional pressure sensors, to pressure variation with a higher frequency than the cutoff frequency, while it outputs a less signal for a lower frequency. The cutoff frequency must be set below the principal frequencies of the pressure variation of the measuring object. Since the cutoff frequency is determined by the duration of the induced pressure difference, the duration is a significant parameter in designing the sensor. So, it is worthwhile to clarify the relationship between the duration of the induced pressure difference and the dimensions of the semi-closed space.

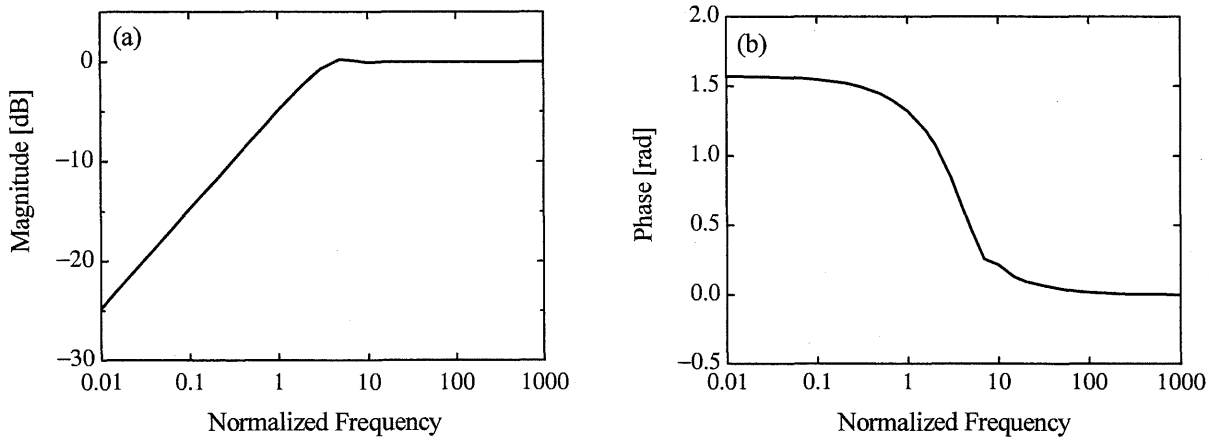

Fig. 3 The calculated magnitude and phase of the transfer function of the sensor as a function of the normalized frequency f/f_0 . f_0 is defined as the reciprocal of the duration of the induced pressure difference.

4. EXPERIMENT

4.1 Fabrication

Figure 4 shows the top and cross-sectional views of the fabricated sensor, including the actual dimensions. The sensor, except for the bottom plate, was built using two glasses: a Corning #0211 glass as a diaphragm plate and a soda-lime glass with a 14 mm× 14 mm square hole to support the diaphragm plate. First, a thin aluminum film was evaporated on a Corning glass. The aluminum film was removed using a patterned photoresist mask. Next, the glass was immersed in pure KNO_3 for two hours at 400 °C to form the single-mode channel waveguides. Before the two substrates were fixed, the waveguide was adjusted to be parallel to the diaphragm. Then, both substrates were bonded together by UV adhesion. Finally, a plate with a small hole was attached to the bottom as shown in Fig. 4.

The diaphragm dimensions were 14 mm× 14 mm× 0.22 mm, and the volume of the semi-closed space was 14 mm× 14 mm× 1.8 mm. The diameter of the small hole was 0.05 mm (Sensor #1), 0.1 mm (Sensor #2), and 0.8 mm (Sensor #3).

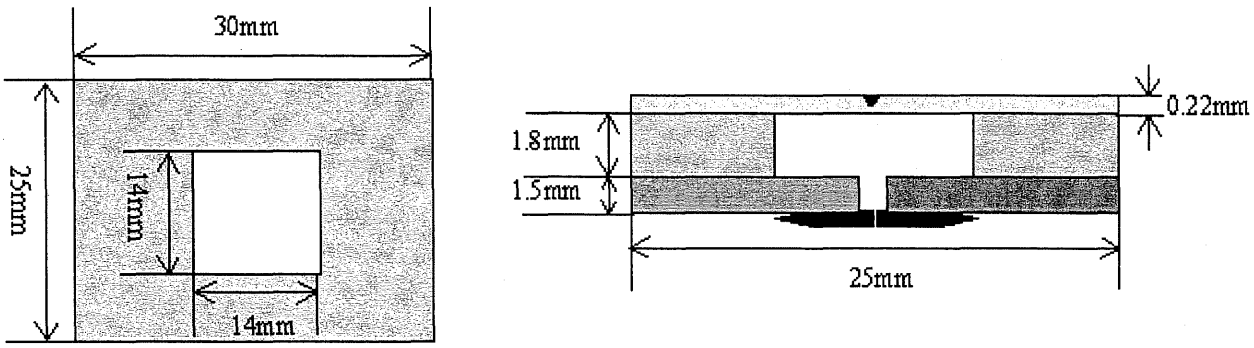

Fig. 4 (a) Top and (b) cross-sectional views of the fabricated sensor, including the actual dimensions.

4.2 Measurement

Figure 5 shows the experimental setup to measure the output power in a step-like pressure change. In the experiment, a linearly-polarized He-Ne laser at 633 nm was used, and its polarization was set at 45° with respect to the sensor surface. The fabricated sensor was placed in the closed box with a volume of 30 cm × 28 cm × 30 cm. The closed box has ports connected to a vacuum pump and to a leak valve. In addition, the pressure gauge was mounted on the closed box to monitor pressure in the box.

Figure 6 shows the pressure sequence in the closed box and an example of expected outputs. After monitoring the initial output power of the sensor, the closed box is gradually decompressed by the vacuum pump at a rate less than –0.5 kPa/sec. When the pressure in the closed box drops to a range from –2 kPa to –5 kPa, decompression is stopped. After stopping decompression, the pressure in the closed box slowly increases due to undesirable air leaking. Such a pressure rise does not interfere with the balance of the pressures in the closed box and in the semi-closed space of the sensor since its rising rate is relatively low. When the pressure of the closed box reaches at 1 kPa, the leak valve is opened so that the pressure change by 1 kPa is applied to the sensor. The ideal output changes for a short while only after the step-like pressure change as shown in Fig. 6(a).

The experimental results of the fabricated sensors are shown in Figs. 7-9. As mentioned above, the pressure in the closed box, that is, the surrounding pressure of the sensor, was rapidly changed by 1 kPa. It is found from Figs. 7 and 8 that the outputs change after the step-like pressure change as expected. For Sensors #1 and #2, the duration of the induced pressure difference was approximately 150 sec and 50 sec, respectively. Regarding Sensor #3, the area of the small hole was so large that the duration was not measured. The measured durations are larger by a factor of thousands than the theoretical ones, 0.060 sec for Sensor #1 and 0.015 sec for Sensor #2. The difference is attributed to pressure drop and fluid friction at the small hole of the semi-closed space. Moreover, according to the theoretical analysis, the duration is inversely proportional to the cross-sectional area of the small hole. Regarding Sensors #1 and #2, the theoretical ratio of the duration is 4:1, while the experimental one is 3:1. The theoretical and experimental ratios are close each other. Hence, the theoretical model gives good indication of the qualitative properties of the sensor.

Incidentally, during decompression in the closed box, the output unexpectedly drops to around 0. This may be caused by an induced misalignment of the optical system in the closed box. Such a misalignment does not disturb measurement of the duration of the induced pressure difference since a quick recovery of the output to the initial value was confirmed for a sensor without a semi-closed space.

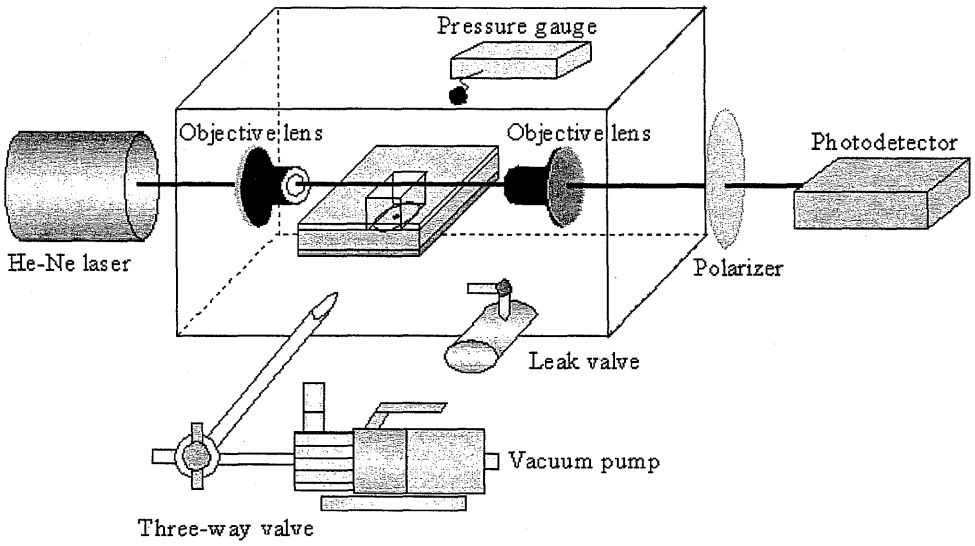

Fig. 5 Experimental setup to measure output power in a step-like pressure change in the closed box. A sensor and two objective lenses were put in a closed box.

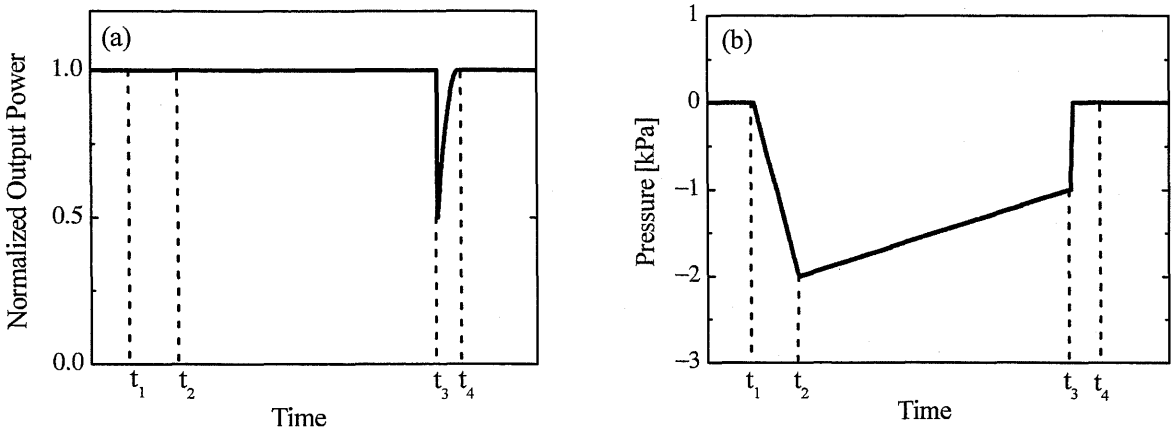

Fig. 6 (a) An example of expected outputs, and (b) a pressure sequence in the closed box in which the sensor is placed as shown in Fig. 5.

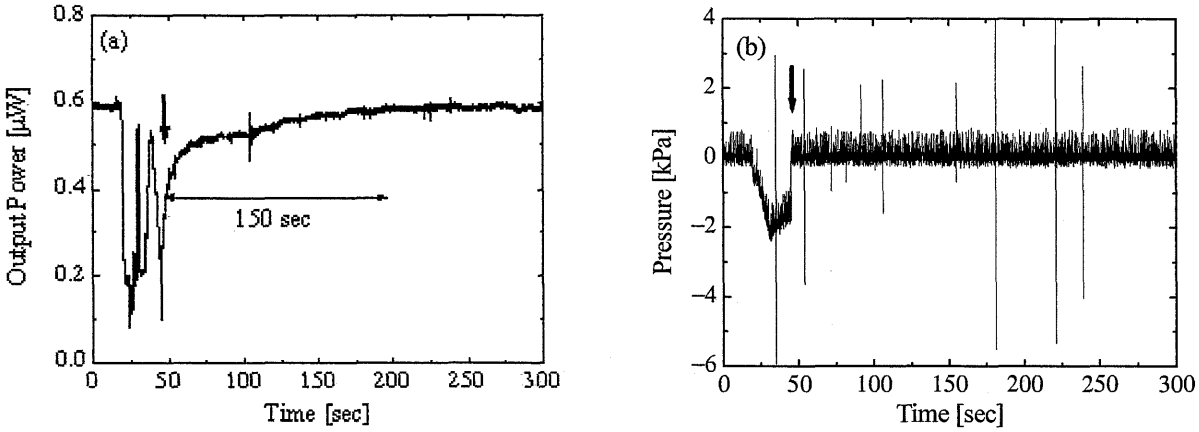

Fig. 7 (a) Measured output power for Sensor #1, and (b) pressure change in the closed box as a function of time. The arrows show the time when the step-like pressure change was applied.

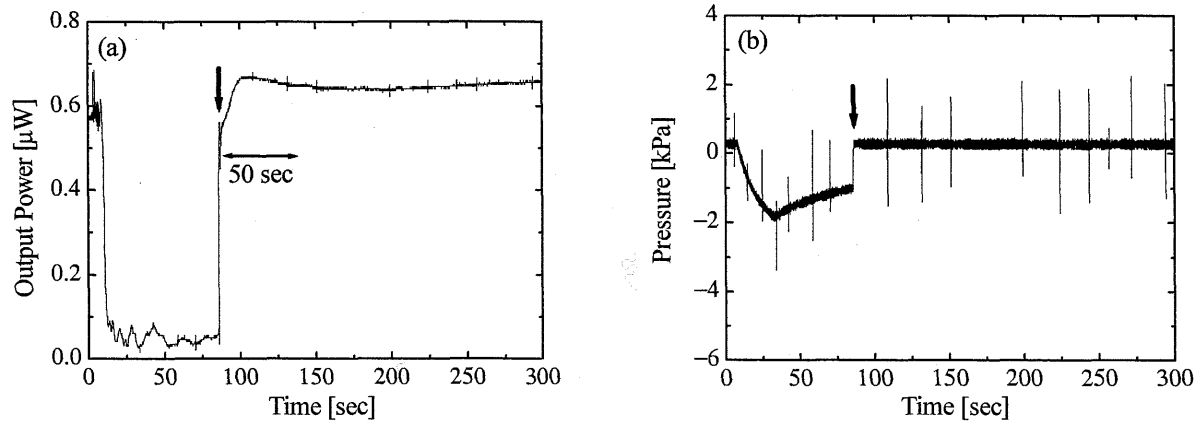

Fig. 8 (a) Measured output power for Sensor #2, and (b) pressure change in the closed box as a function of time. The arrows show the time when the step-like pressure change was applied.

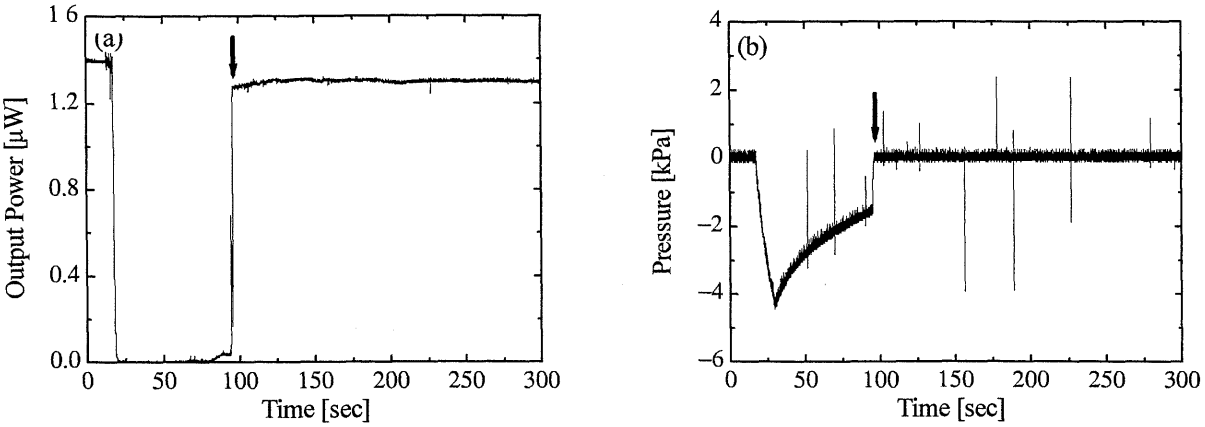

Fig. 9 (a) Measured output power for Sensor #3, and (b) pressure change in the closed box as a function of time. The arrows show the time when the step-like pressure change was applied.

5. CONCLUSIONS

The original guided-wave optical pressure sensor has good feasibility to detect pressure fluctuation even under extremely high pressure since high sensitivity is compatible with high proof pressure by introducing a semi-closed space with a small hole. In this study, the step response in relation to the area of the small hole was examined experimentally. The measured durations were larger by a factor of thousands than the calculated ones. This may be caused by a pressure drop and fluid friction at the small hole. So, these effects must be reflected in the theoretical model. Moreover, since there is insufficient data, experimental data must be collected in order to discuss the design of the sensor and to improve the theoretical model. Although it has not yet been confirmed that the sensor has high proof pressure under static pressure, the sensor would be appropriate for the following applications: monitoring for malfunction in static-high-pressure pipelines of industrial plants, observation of tidal waves which cause hydraulic pressure change on the bottom of the sea, etc.

ACKNOWLEDGEMENTS

We would like to thank Mr. Y. Nozawa for his invaluable help in the experiment. This work is supported in part by a Grant-in-Aid for Scientific Research (No.17360157) from the Japan Society for the Promotion of Science.

REFERENCES

1. L. M. Johnson, G. W. Pratt, and F. J. Leonberger, "Integrated-optical temperature sensor," *in Technical Digest, Third International Conference on Integrated Optics and Optical Fiber Communication* (Washinton, DC, 1981), paper WL4.
2. A. Yamada, T. Tokita, M. Ohkawa, S. Sekine, and T. Sato, Proc. SPIE, **4987**, pp. 248-255, 2003.
3. Y. Iwase, Y. Okamoto, M. Ohkawa, S. Sekine, and T. Sato, Proc. SPIE, **4987**, pp. 256-263, 2003.
4. G. N. De Brabander, Glenn Beheim, and J. T. Boyd, "Integrated optical micromachined pressure sensor with spectrally encoded output and temperature compensation," Appl. Opt., **37**, pp. 3264-3267, 1998.
5. H. Porte, V. Gorel, S. Kiryenko, J. Goedgebuer, W. Daniau, and P. Blind, "Imbalanced Mach-Zehnder interferometer integrated in micromachined silicon substrate for pressure sensor," J. Lightwave Technol., 17, pp. 229-233, 1999.
6. Y. Endo, M. Ohkawa, S. Sekine, and T. Sato, Proc. SPIE, **5728**, pp.309-316, 2005.